Chapter 3

STUDY OF REGULARIZED STATISTICAL APPROACHES FOR CT/PET/SPECT IMAGE RECONSTRUCTION

In this chapter, various regularization priors have been studied and focus on improving statistical iterative reconstruction algorithms by incorporating a suitable prior knowledge of the object being scanned. This chapter is divided into the following sections and sub-sections. Section 3.2 formulates the backgrounds of reconstruction problem and introduces some notations of the EM method. Sub-Section 3.3 describes the proposed hybrid method using fusion of regularization term AD with MLEM. Sub-Section 3.3.1 presents the first proposed model based on the selection of priors for SIR method with their result and analysis discussion. Sub-section 3.3.2 presents the second proposed a new PDE based EM model adapted to poisson noise for medical image reconstruction their result and analysis discussion. Section 3.4 presents the overall discussion about simulation and results of both the proposed models with their qualitative and quantitative analysis and in the last section 3.5, final conclusion of this chapter are presented.

3.1. Introduction

Medical image reconstruction algorithms play a significant role in the image quality by using spatial regularization that penalizes image intensity difference between neighboring pixels. In literature many image reconstruction algorithms have been described for CT/PET (Qi J *et. al.,* 2006). Statistical image reconstructions (SIR) algorithms substantially improve the image quality as compared to the conventional filtered back-projection (FBP) method (J. Devaney, 1982) for various clinical tasks. SIR based maximum likelihood expectation maximization (MLEM) algorithm (Shepp and Vardi, 1982) produces images with better quality than analytical techniques. It can better use of noise statistics, accurate system modeling, and image prior knowledge. MLEM estimates the objective function that is being maximized (log-likelihood) when the difference between the measured and estimated projection is minimized. There have been further refinements of the SIR with introduction of ordered subset expectation maximization (OSEM) (Hudson and Larkin, 1994) that uses a subset of the data at each iteration, thereby producing a faster rate of conversion.

Although, likelihood increases, the images reconstructed by classical MLEM are still very noisy because of ill-posed nature of SIR algorithms. During reconstruction process, poisson noise effectively degrades the quality of reconstructed image. Regularization is therefore required to stabilize image estimation within a reconstruction framework to control the noise propagation and to produce a reasonable reconstruction. Generally, the penalty term is chosen as a shift-invariant function that penalizes the difference among local neighbouring pixels. The regularization term incorporates prior knowledge or expectations of smoothness or other characteristics in the image, which can help to stabilize the solution and suppress the noise and streak artifacts. Various regularizations have been presented in the past decades based on different assumptions, models and knowledge. Although some of them were initially proposed for SIR of CT, they can be readily employed for PET. This regularization term is used to stabilize the image estimation. To incorporate prior knowledge or expectations of smoothness in the image, which encourage preservation of the piecewise contrast region while eliminating impulsive noise, but the reconstructed images still suffer from streaking artifacts and poisson noise.

Numerous edge preserving priors have been proposed in the literature (Chen Y *et. al.,* 2006; Denisova NV *et.al.,* 2004; Chlewicki W *et. al.,* 2004; Perona and Malik, 1990; Rajeev Srivastava *et. al.,* 2013; Liang Z *et. al.,* 1989; Nunez J *et. al.,* 1990; Fessler, 2006; Herman and Levitan, 1987; Chen G-H *et. al.,* 2008; Chun I Y *et. al.,* 2013; Kang D *et. al*. 2013; Wang G *et. al.,* 2012; Z. G. Gui *et. al.,* 2012; D. Kazantsev *et. al.,* 2012) to produce sharp edges while suppressing noise within boundaries. A wide variety of methods such as the quadratic membrane (QM) (Chen Y *et. al*., 2006) prior, Gibbs prior (Geman and Geman, 1984), entropy prior (Denisova NV *et.al.*, 2004; Liang Z *et. al.,* 1989; Nunez J *et. al.,* 1990), Huber prior function (Chlewicki W *et. al.,* 2004), Compressed sensing (CS) based prior (Chun I Y *et. al.,* 2013), Total Variation (TV) prior (Panin VY *et. al.,* 1999), Block-Matching 3D (BM3D) (Kang D. *et. al.,* 2013), Probabilistic Patch Based prior (PPB) (Wang G *et. al.,* 2012), and Anisotropic Diffusion (AD) (Perona and Malik, 1990) etc. regularization priors are used as a penalty function in previous studies. In order to suppress the noise and preserve edge information simultaneously, image reconstruction based on AD has become the interesting area of research (Z. G. Gui *et. al.*, 2012; D. Kazantsev *et. al.*, 2012; Qian He *et. al.*, 2014; Hsiao I-T *et. al.,* 2003). Zhi-guo Gui and Jiawei He, proposed a regularized maximum likelihood algorithm (Z. G. Gui *et. al.*, 2012) that combined MLEM with AD filter during post-processing reconstruction (named PML_NewAD) and could obtain acceptable reconstructed results. However, PML_NewAD cannot remove the isolated noise and preserve edge information accurately due to the defects of P-M diffusion model (D. Kazantsev *et. al.*, 2012). Qian He and Lihong Huang also follow the same trends and proposed (named PML_AMD) (Qian He *et. al.*, 2014) that combined median AD with MRP during post-processing.

Here in this chapter, we introduces and evaluates a hybrid approach to regularize which dominate in CT/PET images. Our model is looking equivalent to that proposed in (Z. G. Gui *et. al.*, 2012), and (Qian He *et. al.*, 2014) but it's different in the sense that we focus on edge-preserving regularizer (AD) with MLEM i.e. (MLEM+AD), which produces fast reconstructed results in an efficient manner. However, unlike (Z. G. Gui *et. al.*, 2012; Qian He *et. al.*, 2014) which treat post-processing reconstruction steps our approach is based on an elegant formulation that use priors (filters) within the reconstruction process rather than using at the end after the reconstructed image is ready.

3.2. Background

Maximum likelihood Expectation Maximization (MLEM) has become one of the most widely used iterative methods for CT/PET reconstruction (Qi J *et. al.*, 2006, Fessler, 2006; Herman and Levitan, 1987; Lange K *et. al.,* 1987). The significant merit of this algorithm is that it can achieve much better quality images with lesser number of views needed in FBP (J. Devaney, 1982).Here a standard model of photon emission tomography as described in (Qi J *et. al.*, 2006) is used and the measurements follow independent Poisson random distribution as follows:

$$y_i \sim Poisson\left(\bar{y}_i(f)\right), i = 1, ..., I \tag{3.1}$$

where y_i is the measured projectional data which are counted by the i^{th} detector during the data collection, f represents the estimated image vector and the element of f denotes the activity of image. In iterative methods, the calculation of the system matrix during the reconstruction process is essential and given as follows:

$$\bar{y}_i(f) = \sum_j^J a_{ij} f_j \tag{3.2}$$

where, $A = \{a_{ij}\}$ is the weight matrix or system matrix which represents the probability of an event in pixel *i* being detected by LOR (Line Of Response) *j*. System matrix is a key factor in MLEM algorithm which models the relationship between the measured projection data and the estimated image vector. The probability distribution function *(pdf)* of the Poisson noise reads:

$$P(y|f) = \prod_i^I \frac{\bar{y}_i(f)^{y_i}}{y_i!} \exp\left(-\bar{y}_i(f)\right), \tag{3.3}$$

and the corresponding log-likelihood can be described as follow:

$$L(f) = \log P(y|f) = \sum_{i=1}^{I}\left(y_i \log\left(\sum_{j=1}^{J} a_{ij} f_j\right) - \sum_{j=1}^{J} a_{ij} f_j\right) \tag{3.4}$$

where I is the number of detector pairs, J is the number of the objective image pixels, and $P(y|f)$ is the probability of the detected measurement vector y with image intensity f.

The formula of MLEM algorithm can thus be described as:

$$f_j^{(k+1)} = \frac{f_j^{(k)}}{\sum_{i=1}^{n} a_{ij}} * \sum_{i=1}^{n} \frac{y_i a_{ij}}{\sum_{j=1}^{m} a_{ij} * f_j^k} \tag{3.5}$$

where $f_j^{(k+1)}$ is the updated image after $(k+1)^{th}$ iteration. Although, MLEM algorithm is better than filtered back-projection (FBP) algorithm (Shepp and Vardi, 1982), its major problem is that different features converges at different speeds, and as the number of iteration increases, they tend to computationally intensive. Additionally, MLEM algorithm is also ill-posed. To deal with the issue of ill-posedness nature of MLEM, various edge preserving regularization priors have been proposed in the literature (Wang G *et.al.,* 2012; Z. G. Gui *et. al.*, 2012; D. Kazantsev *et. al.,* 2012; Qian He *et. al.,* 2014; Hsiao I-T *et. al.,* 2003) to produce sharp edges while suppressing noise within boundaries.

Further, we propose to incorporate a regularization function in the above reconstruction problem Eq. (3.5) to remove noise and blur in an images, while preserving edges (Rajeev *et. al.,* 2013; Hsiao I-T *et. al.,* 2003). This can be achieved by casting the reconstructed problem adapted to poisson noise by the following general optimization framework as:

$$\hat{f} = \arg\max_{f \geq 0} \left(L\left(y|f\right) - \beta U\left(f\right) \right) \tag{3.6}$$

where $U(f)$ is the image roughness penalty. Conventionally the image roughness is measured based on the intensity difference between neighboring pixels:

$$U\left(f\right) = \sum_{j} \sum_{k \in W_j} w_{jk} \phi\left(f_j - f_k\right) \tag{3.7}$$

where $\varphi(t)$ is the penalty function. The regularization parameter β controls the trade-off between data fidelity and spatial smoothness. When β goes to zero, the reconstructed image approaches the ML estimate. The main reason for the instability of traditional regularizations is that the image roughness is calculated based on the intensity differences may not be reliable in differentiating sharp edges from random fluctuation due to noise. When the intensity values contain noise, some possible choices of penalty function $\varphi(t)$ are categorized as follows: A common choice of $\varphi(t)$ in PET image reconstruction is the quadratic function:

$$\varphi(t) = \frac{1}{2}t^2 \tag{3.8}$$

A disadvantage of the quadratic prior (Chen Y *et. al.*, 2006) is that it may over-smooth edges and small objects when a large β is used in order to smooth out noise in large regions.

The second type of independent prior is based on the entropy function (Denisova NV *et.al.*, 2004), whose corresponding energy function *U (μ)* can be described as:

$$\varphi(t) = \sum_j t_j \ln t_j \tag{3.9}$$

Basically, these two priors have the tendency to smooth both high-frequency edge regions and low-frequency background, so they cannot explicitly enforce smoothness in the image (Fessler, 2006).

The third type of independent prior is the Gaussian prior (Levitan and Herman, 1987), whose energy function has the form:

$$\varphi(t) = \sum_j \frac{\left(t_j - \bar{t}_j\right)^2}{2\sigma_j^2} \tag{3.10}$$

where t_j and σ_j^2 are the mean and variance respectively, and when $\bar{t}_j = 0$ it reduces to Eq. (3.8).

Similarly, the Gamma prior (Lange K *et. al.*, 1987) allows only non-negative image values and can be a more natural model for an image:

$$\varphi(t) = \sum_j \rho\left(t_j, \bar{t}_j, \sigma_j\right) \tag{3.11}$$

where $\rho\left(t_j, \bar{t}_j, \sigma_j\right)$ is a Gamma PDF.

Basically, the Gaussian and Gamma priors encourage the neighbouring pixel values to be close to the mean image. Thus, the determination of the mean image has a significant effect on the reconstructed image. Some researchers investigated a new approach to estimate the mean image during the reconstruction using either the median or the mean of neighbouring pixels. However, in these cases, the priors are no longer truly independent.

Another form of priors assumes that the attenuation maps are locally smooth, i.e., the neighbouring pixels tend to have similar values. One simple mathematical model that can describe this property is the Markov random field (MRF) model, also known as Gibbs distribution (Geman and Geman, 1984):

$$P(f) = \frac{1}{Z}\exp\left[-\beta U(f)\right] \tag{3.12}$$

where Z is a normalizing constant, and the Gibbs energy *U(f)* is a weighted sum of potential functions (Wernick, 2004):

$$U(f) = \sum_j {}_{m_1, m_2, m_3 \ldots \in W_j} \sum w_{m_1 m_2 m_3 \ldots} \phi\left(f_{m_1}, f_{m_2}, f_{m_3}, \ldots\right) \tag{3.13}$$

where W_j represents the MRF window of the *j*th pixel, and pixels indexed by *m1, m2, m3, ...*, are the neighbouring pixels within the MRF window; *m1,m2,m3 ... w* denotes the weighting coefficient (indicating interaction degree) among the pixels; and ϕ denotes a positive potential function. The choice of potential function is very critical since it strongly determines the smoothness properties of the MAP estimate. One common choice of ϕ in image reconstruction is the quadratic function, $\phi(\Delta) = \Delta^2/2$, and in this case, Eq. (3.13) becomes:

$$U(f)=\sum_{j}\sum_{m\in W_j} w_{jm}\frac{1}{2}\left(f_j-f_m\right)^2 \tag{3.14}$$

which corresponds to the Gaussian MRF (GMRF) prior (Yuxiang Xing *et. al.,* 2004) that has been widely used for SIR. A major drawback of the GMRF prior is that it can excessively penalize the differences between neighbouring pixels when f_j and f_m fall across a discontinuous boundary in the image, thus may lead to over smoothing of edges and fine structures in the reconstructed image. To mitigate this issue, some researchers replaced the quadratic potential function with non-quadratic functions that increase less rapidly for sufficiently large differences. In this way, the corresponding priors are expected to remove noise while retaining sharp edges in the reconstructed image.

Another family of convex function prior is q-generalized Gaussian MRF prior (q-GGMRF) (18), which can be described as:

$$\phi(\Delta)=\frac{|\Delta|^p}{1+|\Delta/\delta|^{p-q}}\ \left(1\le q\le p\le 2\right) \tag{3.15}$$

By giving specific parameter values, it can become:

$$\phi(\Delta)=\begin{cases}\Delta^2, \left(q=p=2, \textit{Gaussian prior}\right)\\ |\Delta|, \left(q=p=1, \textit{median pixel prior}\right)\\ |\Delta|^p, \left(1<q=p\le 2, \textit{generalized Gaussian MRF}\right)\\ \dfrac{\Delta^2}{1+|\Delta/\delta|}, \left(q=1, p=2, \textit{approximate Huber prior}\right)\\ \dfrac{\Delta^p}{1+|\Delta/\delta|^{p-q}}, \left(1\le q<p\le 2, q-\textit{generalized Gaussian MRF}\right)\end{cases} \tag{3.16}$$

In Median root Prior (MRP), intensity differences among neighboring pixels are not penalized. Instead, the penalty is set according to how much the central pixel differs from the local median. Mathematically, the MRP can be described as (Alenius S, Ruotsalainen, 1989):

$$U(f)=\sum_{j}\frac{\left(f_j-median\left(f_j\right)\right)^2}{median\left(f_j\right)} \tag{3.17}$$

where $median(f_j)$ is the local median. Therefore, no penalty is applied when the image is locally monotonic, and only non-monotonic local changes among neighbouring pixels are penalized. Although the MRP captures significant edges while encouraging preservation of locally monotonic regions, it is a heuristic empirical method and not convex in theory.

Recently, a new signal reconstruction theory, compressed sensing (CS) (Chen G-H *et. al.*, 2008; Chun I Y *et. al.*, 2013), has been rigorously formulated to accurately reconstruct a signal from much fewer samples than that is required by the Nyquist sampling theorem (Candes E J *et. al.*, 2006). The main idea of CS is that most signals are sparse in appropriate orthonormal systems, that is, a majority of their coefficients are close or equal to zero. Researchers tried to apply this theory to accurately reconstruct CT images at a much lower angular-sampling rate than the Nyquist sampling, but the CT images are generally not sparse in their original pixel representation (Chun I Y *et. al.*, 2013).

Mathematically, the CS method reconstructs an image via the L_p norm ($0 \le p < 2$) minimization. Herein, for a vector θ, $||\theta||_0$ represents the L_0 norm of vector θ which counts the number of nonzero components of θ, and $||\theta||_p$ (p > 0) denotes the L_p norm of vector θ which is defined as:

$$\|\theta\|_p = \left(\sum_j |\theta_j|^p\right)^{1/p} \quad \rightarrow \quad \|\theta\|_p^p = \sum_j |\theta_j|^p \tag{3.18}$$

It should be noted that $||\theta||_p$ is not actually a norm when $0 \le p < 1$ because it is not sub-additive, yet we still refer it as norm following convention (sort of abuse of terminology).

The next choice is total-variation (TV) which is widely used penalty function in image reconstruction that avoids smoothing of salient details (Panin VY *et. al.*, 1999), which is given as the 1-norm of the gradient of the solution. Regularization with the TV penalty results in smoothing of weakly varying details and preservation of salient (having strong variation) details such as edges:

$$\varphi(t) = \sqrt{t + T^2} - T \tag{3.19}$$

where, T is a thresholding parameter. Another methods to reduce the amount of noise present in the images, we used a high performance spatially adaptive Block matching 3D filter (BM3D), (Kang D *et. al.*, 2013) which is used for the noise removal. BM3D is based on the assumption that a noise-free image spectrum of similar image fragments group can be better approximated as a combination of a few spectrum elements than a single image fragment (Wang and Qi, 2012), proposed a patch-based regularizations.

Traditional regularizations penalize image roughness based on the intensity difference between neighboring pixels, but the pixel intensity differences may not be reliable in differentiating sharp edges from random fluctuation due to noise. To address this issue, (Wang and Qi 2012) proposed patch-based regularizations which utilize neighborhood patches instead of individual pixels to measure the image roughness. Since they compare the similarity between patches, the patch-based regularizations are believed to be more robust in distinguishing real edges from noisy fluctuation. The patch-based roughness regularizations are defined as:

$$U(f)=\sum_{j=1}^{n_j}\sum_{k\in SW_j} w_{jk}\varphi\left(\left\|g_j(f)-g_k(f)\right\|_{2,c}\right) \qquad (3.20)$$

where $w_{jk}=1$, or $w_{jk}=1/d_{jk}$ and $g_j(f)$ and $g_k(f)$ is the feature vector consisting of intensity values of all pixels in the patch centered at pixel *j* and *k* respectively.

3.3. Proposed Models

In this section, a new hybrid framework (here referred to as: MLEM+AD) to reduce number of iterations as well as to improve the quality of reconstructed images is proposed. This method speedup the reconstruction process using a statistical EM algorithm called maximum likelihood expectation maximization (MLEM). Additionally, nonlinear partial differential equation (PDE) based diffusion process, anisotropic diffusion (AD) prior (Perona and Malik, 1990), is combined to maximize the likelihood function. The proposed method solves computational time, slow convergence as well as ill-conditioned problem of iterative methods. Numerical simulation experience demonstrates that proposed penalized reconstruction algorithm is superior to the MLEM without prior and MLEM with QM, Huber, TV, BM3D, PPB priors.

Finally, hybrid method is applied to CT/PET tomography for obtaining optimal solutions. Generally, the SIR methods can be derived from the maximum a posteriori (MAP) estimation, which can be typically formulated by an objective function consisting of two terms named as “data-fidelity” term, models the statistics of projection measurements, and “regularization” term, penalizes the solution. It is an essential criterion of the statistical iterative algorithms that the data-fidelity term provides an accurate system modeling of the projection data. The regularization or penalty term play an important role in the successful image reconstruction. Further, the next section presents, penalizaed or regularized maximum likelihood reconstruction algorithm using various choice and evaluation of priors for CT/PET.

3.3.1. On the choice and evaluation of regularization priors in penalized maximum-likelihood image reconstruction for CT/PET

Computed Tomography and Positron Emission Tomography (CT/PET) is an effective and indispensable imaging tool. The noise contained in the data measured by imaging instruments is primarily Poisson type and decreasing the noise has the potential to optimize the quality of CT/PET images. In this section, anisotropic diffusion (AD) prior based maximum-likelihood expectation maximization (MLEM) method is proposed for the reconstruction of CT/PET images from noisy projection data. The proposed method is well capable of dealing with the problem of ill-posedness arising due to sole use of MLEM algorithm. Further, this section investigates and presents the quantitative analysis of various priors available in reconstruction literature to deal with the problem of ill-posedness and makes a recommendation for selecting an appropriate prior to be used with MLEM. The various priors investigated include Quadratic Membrane (QM) prior, Huber Prior, Total Variation (TV) based prior, Block-Matching 3D (BM3D), Gaussian probabilistic patch based prior (PPB), and anisotropic diffusion (AD) based prior. The MLEM based reconstruction method was tested along with the combination of different above mentioned priors one at a time for different phantom test data sets. From obtained results, it is observed that the anisotropic diffusion (AD) based prior with MLEM is performing better in comparison to other priors and produces the good quality reconstructed images.

The proposed hybrid model as shown in Fig.3.1

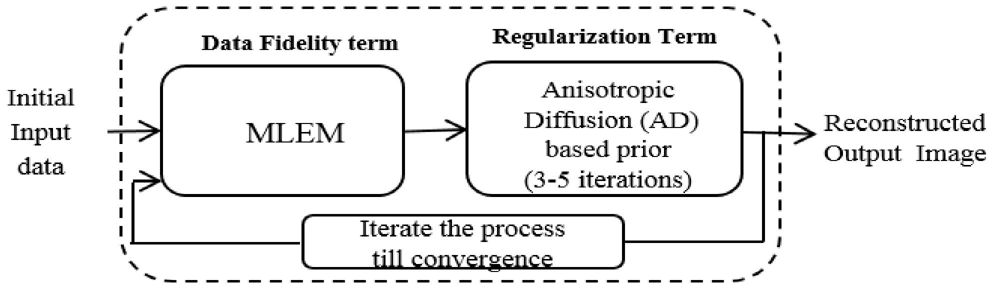

Fig. 3.1: The proposed Hybrid Model

The basic AD equation is:

$$\frac{\partial f}{\partial t} = div\left[C(\nabla f)\nabla f\right] \tag{3.21}$$

where f is the image, t is the iteration step, ∇f is the local image gradient and $C(\nabla f)$ is the *diffusion function,* which is a monotonically decreasing function of the image gradient magnitude, sometimes called the 'edge-preserving' function. The following *diffusion functions* were first proposed by Perona and Malik (1990):

$$C_1(f) = \exp\left[-\left(\frac{\nabla f}{K}\right)^2\right] \quad \text{or} \quad C_2(f) = 1\Big/1+\left(\frac{|\nabla f|}{K}\right)^2 \tag{3.22}$$

where K is a gradient threshold that controls the edge sensitivity of the model. It is a user-specified constant which determines the threshold of the local gradients and controls the edge sensitivity of the filter. However, P-M diffusion model can remove isolated noise and preserve the edges to some extent it cannot preserve the edge details effectively and accurately. To address the limitation of AD method, here we use median filter to the result obtained by AD method (29) in each iteration and the discretised final model is given as follows:

$$f_j^{k+1} = f_j^k + \Delta t \sum_{j' \in N_j} \left(C\left(\left|\nabla f_{j,j'}^k\right|\right)\nabla f_{j,j'}^k\right) \tag{3.23}$$

For the discretized versions of Eq. (3.23) to be stable, the von Neumann analysis (10) shows that we require $\frac{\Delta t}{(\Delta f)^2} < 1/4$. If the grid size is set to $\Delta f = 1$ then Δt < ¼ *i.e.(* Δt *< 0.25)*. Therefore, the value of Δt is set to *0.25* for stability of Eq. (3.23). The proposed hybrid cascade framework is shown in Fig. 1. Towards the end, we refer to the proposed algorithm as an efficient hybrid approach for PET/SPECT image reconstruction and outline it as follows.

Proposed Algorithm: *Reconstruction using MLEM algorithm*

X_{true} *= true projections,* a *= system matrix*

y^n *= updated image after n^th^ MLEM iteration,*

x^n_{calc} *= calculated projections at n^th^ iteration.*

1. Set n = 0 and chose any random image (zero image density or random image density).
2. Calculate Projections: find projections after n^{th} iterations using updated image: $x^n_{calc} = a^T * y^n$

Error Calculation:-Find error in calculated projection (element-wise division)

$$X_{error} = \frac{X_{true}}{x^n_{calc}}$$

Back projection:-Back-project the error onto image

$$X^n_{error} = a * X^n_{error}$$

3. Normalization:- Normalize the error image(element-wise division)

$$X^n_{norm} = \frac{X^n_{error}}{\sum_j a_{ij}}$$

4. Update:- update the image

$$y^{n+1} = y^n .* X^n_{norm}$$

Prior: Use ***AD*** as prior

5. Set m = 0 and apply Anisotropic Diffusion

$$y^{n+1}_{m+1} = AD\left(y^{n+1}_m\right)$$

6. Put m = m+1 and repeat till m = 3;
7. Put n = n+1, repeat with EM reconstruction.

In our algorithm, we monitor the SNR during each loop of secondary reconstruction. The processing is stopped when SNR begins to saturate or degrade from any existing value.

3.3.1.1 Simulation and Results Analysis

To demonstrate the validity of the proposed algorithm (MLEM+AD) we compared the reconstructed images using the proposed algorithm with different algorithm such as MLEM without prior and MLEM with QM, Huber, TV, BM3D, PPB priors in computer simulation. These algorithms were tested by two different computer generated CT phantoms such as modified PET mathematical phantom and standard thorax phantom image as shown in Fig. 3.2. We simulate the sinograms with total counts amount $6x10^5$. The simulated data is all Poisson distributed and all assumed to be 64 radial bins and 64 angular views evenly spaced over 180^0. Projections are calculated mathematically. The standard thorax test image is gray-scale image of size 128x128, with coverage angle ranging from 0 to 360 º with rotational increment of 2 º to 10 º. The resultant reconstructed image obtained from different algorithms is given in Fig. 2 & 5. For simulation study MATLAB 2013b software was used on PC with Intel(R) Core (TM) 2 Duo CPU U9600 @ 1.6GHz, 4.00 GB RAM, and 64 bit Operating system.

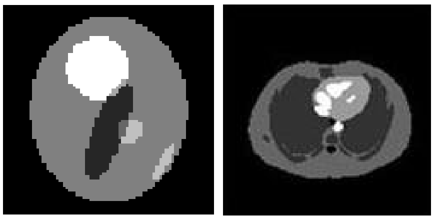

Fig 3.2: Modified Sheep-Logan mathematical phantom (64x64pixels) & Standard thorax medical image (128x128 pixels)

The performance of the proposed hybrid method (MLEM+AD) for image reconstruction defined by Equation (3.23) has been evaluated both qualitatively and quantitatively in terms of various performance measurements metrics such as: signal-to-noise ratio (SNR), the root mean square error (RMSE), the correlation parameter (CP) (Rajeev *et. al.*, 2013), and mean structure similarity index map (MSSIM) (Rajeev *et. al.*, 2013). The SNR and RMSE give the error measures in reconstruction process. The correlation parameter (CP) is a measure of edge preservation in the reconstructed image. The MSSIM is a measure of preservation of luminance, contrast and structure of the image after the reconstruction process, which is necessary for medical images.

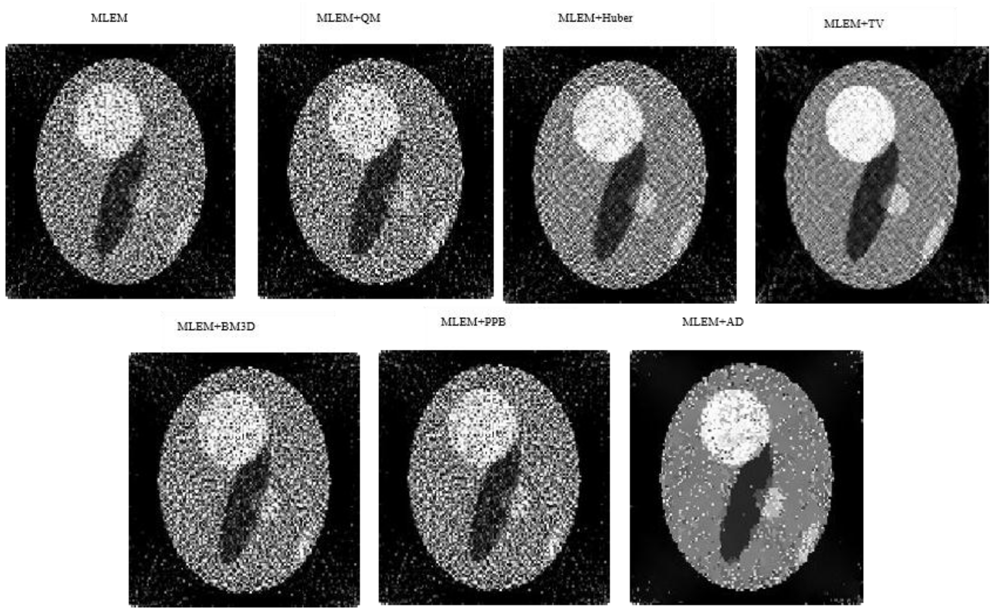

Fig. 3.3: The PET test Phantom with different reconstruction methods. Projection including 10% uniform Poisson distributed background events.

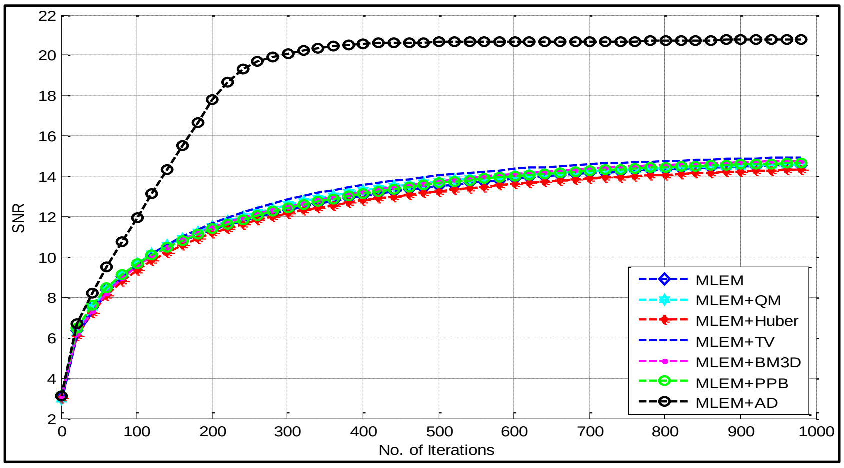

(a)

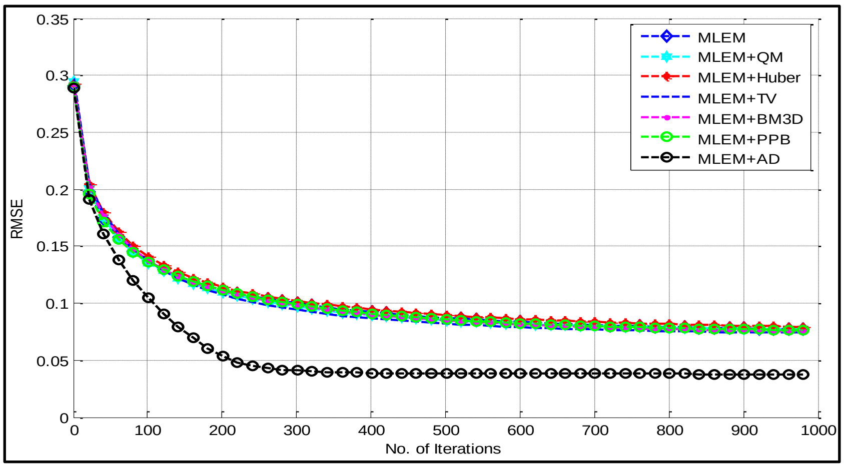

(b)

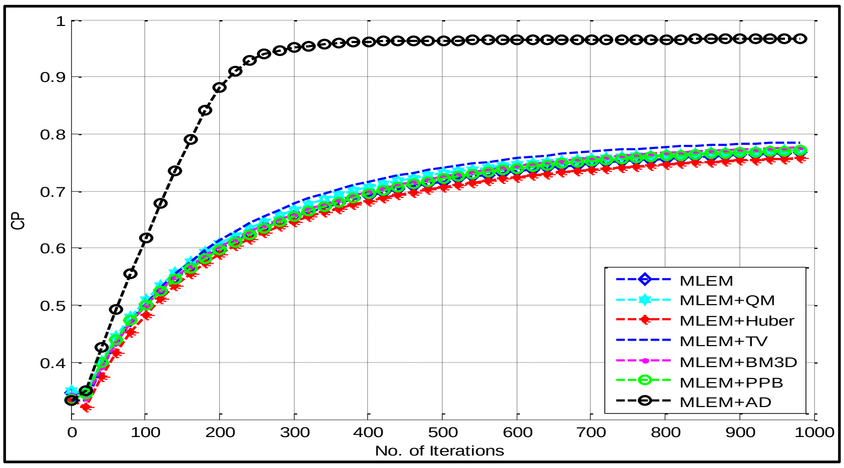

(c)

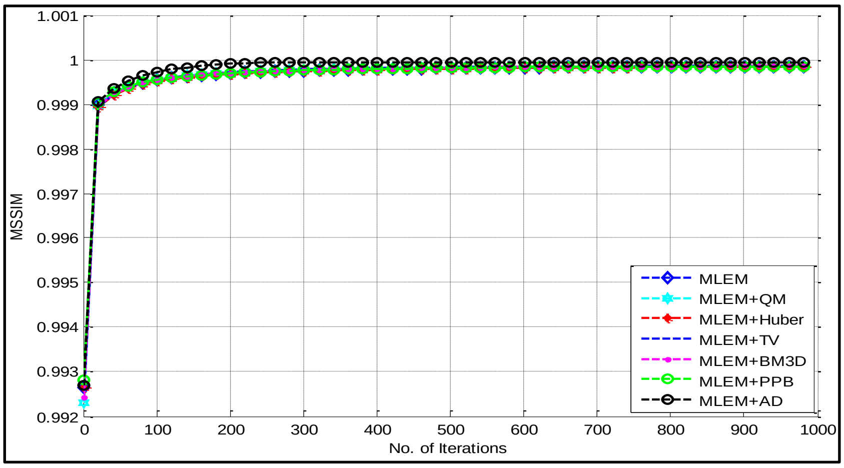

(d)

Fig.3.4: The Plots of (a) SNR, (b) RMSE, (c) CP, and (d) MSSIM along with No. of Iterations for Test case 1.

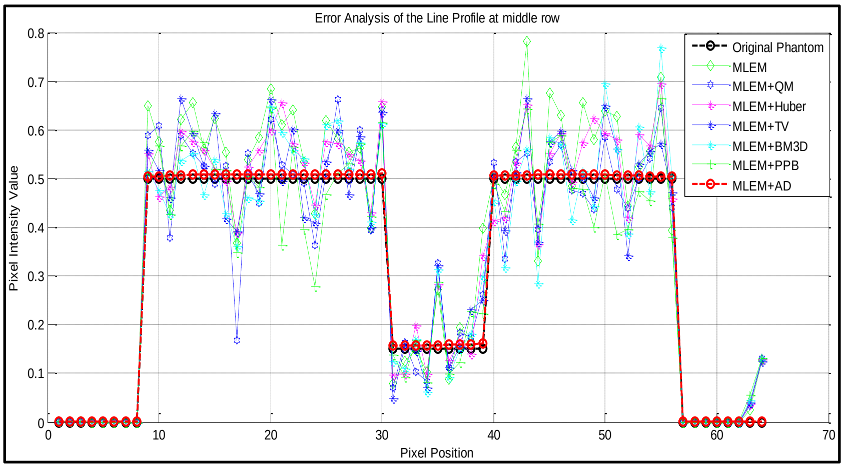

(a)

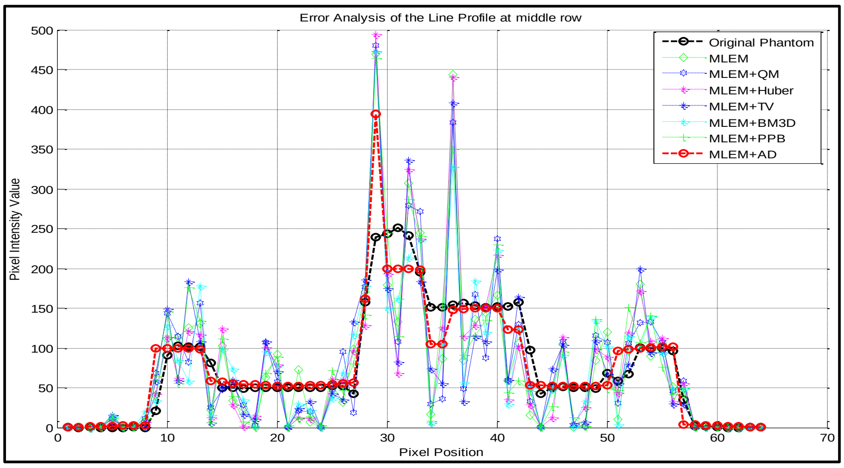

(b)

Fig.3.5: The Line Plots of (a) Shepp-Logan head Phantom and (b) Thorax image

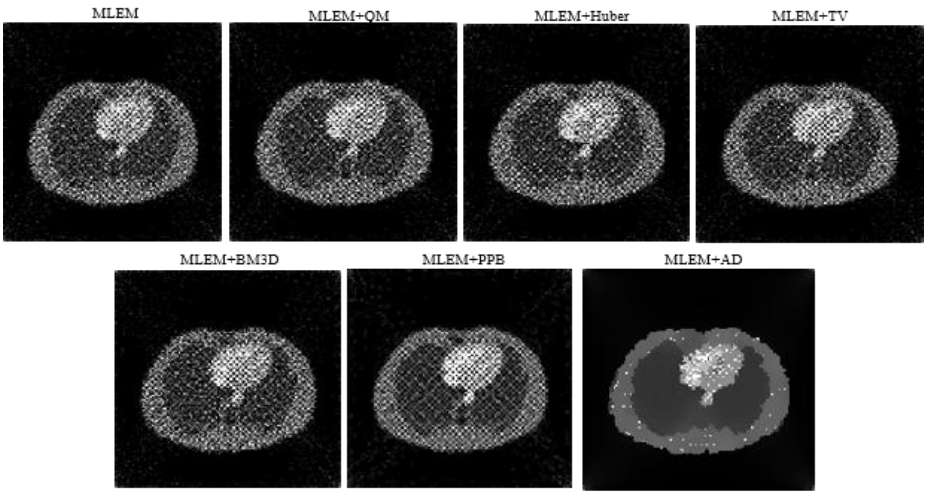

Fig. 3.6: The SPECT elliptical Test Phantom with different reconstruction methods. Projection including 10% uniform Poisson distributed background events.

Table 3.1: Performance measures for the reconstructed images using Proposed (MLEM+AD) and other methods for Test case 1

Performance Measures	**MLEM**	**MLEM +QM**	**MLEM +Huber**	**MLEM +TV**	**MLEM +BM3D**	**MLEM +PPB**	**MLEM+AD (Proposed)**
SNR	14.5846	14.5898	14.3568	14.9474	14.7936	14.6635	20.7875
RMSE	0.0771	0.770	0.791	0.739	0.0752	0.0764	0.0377
CP	0.7675	0.7718	0.7588	0.7860	0.7774	0.7714	0.9671
MSSIM	0.9999	0.9999	0.9998	0.9999	0.9999	0.9999	0.9999

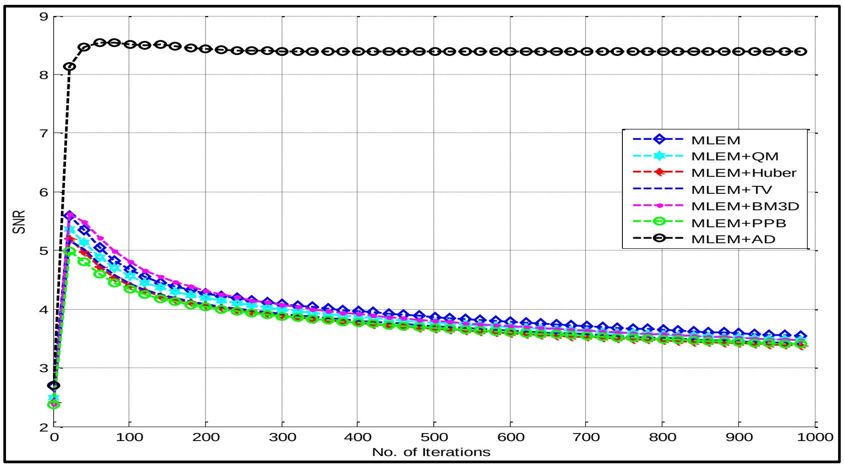
SNR
No. of Iterations
MLEM
MLEM+QM
MLEM+Huber
MLEM+TV
MLEM+BM3D
MLEM+PPB
MLEM+AD

(a)

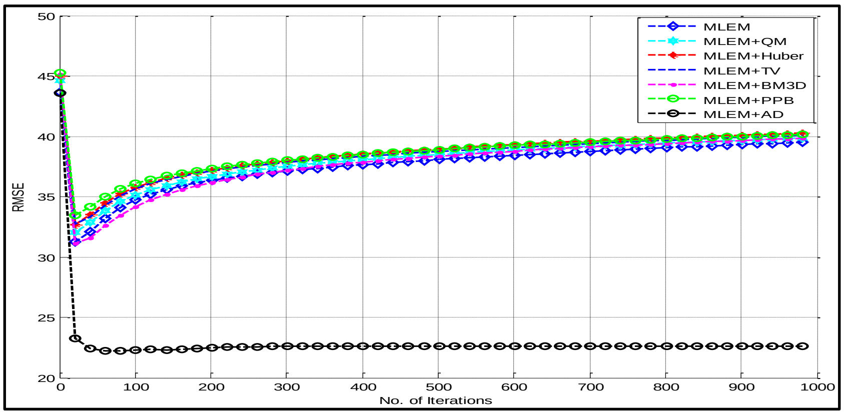
RMSE
No. of Iterations
MLEM
MLEM+QM
MLEM+Huber
MLEM+TV
MLEM+BM3D
MLEM+PPB
MLEM+AD

(b)

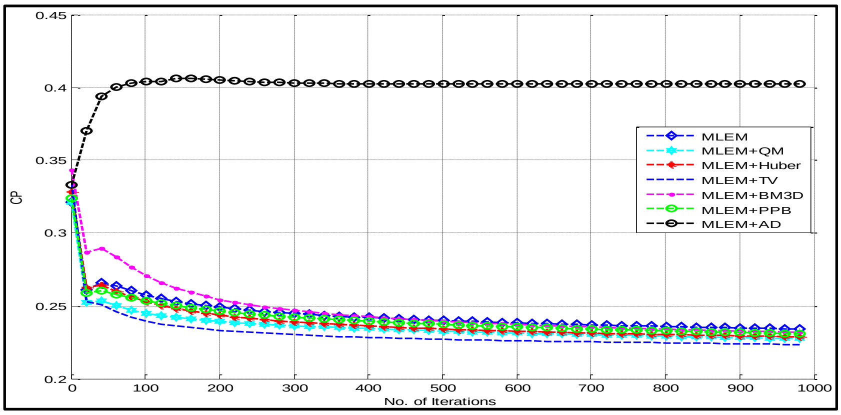
CP
No. of Iterations
MLEM
MLEM+QM
MLEM+Huber
MLEM+TV
MLEM+BM3D
MLEM+PPB
MLEM+AD

(c)

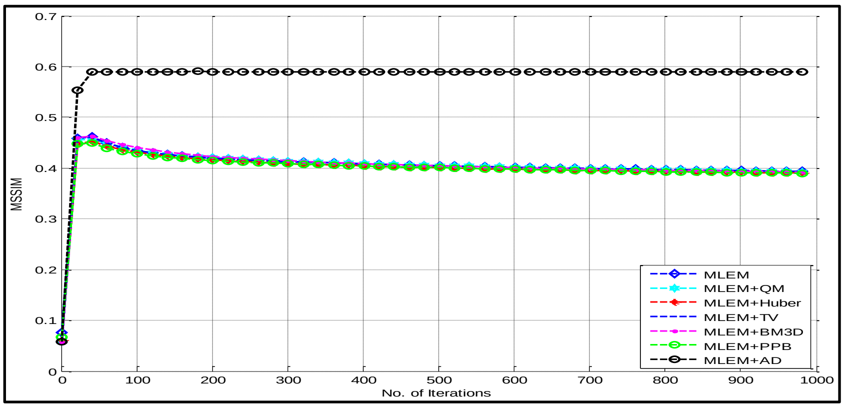

(d)

Fig. 3.7: The Plots of (a) SNR, (b) RMSE, (c) CP, and (d) MSSIM along with No. of Iterations for Test case 2.

Table 3.2: Performance measures for the reconstructed images using Proposed (MLEM+AD) and other methods for Test case 2

Performance Measures	MLEM	MLEM +QM	MLEM +Huber	MLEM +TV	MLEM +BM3D	MLEM +PPB	MLEM+AD (Proposed)
SNR	5.5856	5.3628	5.1948	5.1785	5.6333	4.9893	8.5556
RMSE	31.2321	32.0435	32.6695	32.7307	31.0613	33.4517	22.1871
CP	0.3213	0.3213	0.3282	0.3342	0.3430	0.3239	0.4064
MSSIM	0.4649	0.4611	0.4545	0.4657	0.4662	0.4526	0.5902

For implementation of the proposed method i.e. (MLEM+AD) algorithms Eq. (14) were used. A Poisson noise of magnitude 10% is added to projections. The value of ∇ was set to 0.24 and value of conductivity coefficient k (kappa) was set to 0.033 to 1.0 for different test cases and within each MLEM step, AD is run for 3 iterations. The reconstructed images generated by different algorithms are shown in Fig.3.3 & 3.6. From the figures, we can see that the proposed algorithm has well performance of noise removal and edges preservation especially the thin edges and detail information. At the same time, we can observe that the MLEM+AD algorithm overcomes the shortcoming of streak artifacts and the reconstructed image is more similar to the original phantom.

The algorithm is run for 1000 iterations and graphs are plotted for SNR, RMSE, CP, and MSSIM along with number of iterations for different algorithms are shown in Fig. 3.4 and 3.7 for two different test cases. From Fig. 3.4 and 3.7, it is observed that the SNR values associated with the hybrid method is always higher than that produced by other algorithms such as traditional MLEM without prior and MLEM with QM, Huber, TV, BM3D, PPB priors, which indicates that the hybrid framework significantly improves the quality of reconstruction in terms of SNR. Further it is observed for both the test cases that the proposed method is producing better reconstructed image in (100-150) iterations whereas other methods are taking much higher number of iterations.

Figure 3.4 & 3.7, shows that the RMSE values of proposed method are higher in comparison to other methods which indicate that the proposed method is performing better. Fig. 3.4 and 3.7, show that the CP values of proposed method are higher and close to unity in comparison to other methods which indicate that the proposed method is also capable of preserving the fine edges and structures during the reconstruction process. Fig. 3.4 and 3.7, shows that the MSSIM values of proposed method is higher which indicate that better reconstruction, it also preserves the luminance, contrast and other details of the image during the reconstruction processes. Table 3.1-3.2; shows the quantification values of SNRs, RMSEs, CPs, and MSSIMs. The comparison table indicates that the proposed reconstruction method produce images with prefect quality than other reconstruction methods in consideration.

Figure 3.5, shows the error analysis of the line profile at middle row for the test case. To check the accuracy of the proceeding reconstructions, line plots were drawn, where x-axis represents the pixel position and y-axis represents pixel intensity value. Line plots along the mid-row line through the reconstructions produced by different methods show that the proposed method can recover image intensity effectively in comparison to other methods. Both the visual-displays and the line plots suggest that the proposed model is preferable to the existing reconstruction methods.

In view of above analysis and discussions for above simulation study under consideration it is observed that the proposed hybrid iterative framework converges very fast, producing the better visual results having less reconstruction error, higher SNR values, better edge, structure, luminance, and contrast preservation capabilities in comparison to other standard methods in consideration. In the next section, we propose a PDE based EM algorithms in variational framework adapted to poisson noise for medical image reconstruction.

3.3.2. A PDE based Expectation Maximization algorithm adapted to Poisson noise for Medical Image Reconstruction

The noise contained in the data measured by CT/PET imaging instruments is primarily Poisson type and decreasing the noise has the potential to optimize the quality of CT/PET images. But the traditional iterative reconstruction algorithms of CT/PET cannot effectively filter the noise. Recently anisotropic diffusion (AD) based nonlinear filter is introduced into tomography reconstruction that purports to filter the noise without blurring edges. This section introduces and evaluates a hybrid approach to regularized maximum likelihood expectation maximization (MLEM) iterative reconstruction technique with Poisson variability. Regularization is achieved by penalizing MLEM with Anisotropic diffusion (AD) filter to form hybrid method for CT/PET image reconstruction using partial differential equation (PDE) based variational framework.

The proposed method in which we use the regularization function $\phi(\|\nabla x\|)$ to be an energy function defined in terms of gradient norm of the image. Here we can use the following regularization method was proposed by (Perona & Malik, 1990).

$$\phi(\|\nabla x\|) = \|\nabla x\|^2 \ , \quad (L2\ norm) \tag{3.29}$$

The advantages of this PDE based nonlinear diffusion method is to reduce the noise which encourages the intra region smoothing while reserving the sharp transition between the two different regions. The *anisotropic diffusion penalized poisson maximum likelihood estimation* is obtained by minimizing following:

$$x_\lambda = \arg\min_{u\geq 0}\{T_\lambda(x) = (x - x_O \ln x) + \frac{\lambda}{2}|\nabla x|^2\} \tag{3.30}$$

Therefore, the proposed PDE based model reads as:

$$\begin{aligned} &\arg\min E(x) = \int_\Omega (\alpha \sum_{i=1}^{M} \left((Ax)_i - b_i \log (Ax)_i \right) + \lambda \|\nabla x\|^2 d\Omega, \\ &x_j \geq 0,\ j = 1,....,N, \end{aligned} \tag{3.31}$$

The functional $E(x)$ is defined on the set of $x \in BV(\Omega)$ such that $\log x L^1(\Omega)$ and χ must be positive everywhere.

After applying Euler-Lagrange minimization technique (Rajeev *et.al,* 2012), the Equation (3.31) reads

$$\begin{cases} \min imize \\ \quad x \qquad \int_{\Omega} \|\nabla x\|^2 + \alpha \sum_{i=1}^{M} \left((Ax)_i - b_i \log (Ax)_i \right), \\ subject\, to \end{cases} \tag{3.32}$$
$$x_j \geq 0,\ j = 1,....,N,$$

Using Euler Lagrange minimization for the optimization problem given by Eq. (3.31), the optimality condition is given as follows:

$$\alpha \sum_{i=1}^{M} \left(a_{ij} \left(1 - \frac{b_i}{(Ax)_i} \right) \right) + \nabla.(c(\|\nabla x\|)\nabla x) = 0, \tag{3.33}$$

$y_j \geq 0$, $x_j \geq 0$, $j = 1, \ldots\ldots, N$,

or equivalently

$$\nabla.(c(\|\nabla x\|)\nabla x) + \alpha x_j - \alpha \frac{\sum_{i=1}^{M} \left(a_{ij} \left(\frac{b_i}{(Ax)_i} \right) \right)}{\sum_{i=1}^{M} a_{ij}} x_j = 0 \tag{3.34}$$

After plugging the EM step from Eq.(3.28), the Eq. (11) reads

$$\nabla.(c(\|\nabla x\|)\nabla x) + \alpha x_j - \alpha x_j^{EM} = 0 \tag{3.35}$$

The Final proposed model reads as follows:

$$x_j = x_j^{EM} - \frac{1}{\alpha} \nabla.(c(\|\nabla x\|)\nabla x), \tag{3.36}$$

The second term in Equation (3.36), which is first derivative of log likelihood of Poisson probability distribution function *(pdf)* with respect to estimated image, acts as the data attachment term and measures the dissimilarities at a pixel between observed image and its estimated value obtained during filtering process there by making the whole filtering process adapted to noise.

3.3.2.1 Simulation and Results Analysis

To demonstrate the validity of the proposed algorithm (MLEM+AD) we compared the reconstructed images using the proposed algorithm with different algorithm such as SART, MLEM and MRP in our computer simulation. These algorithms were tested on different computer generated CT phantoms such as modified Shepp-Logan phantom and standard thorax phantom image as shown in Fig. 3.8. We simulate the sinograms with total counts amount $6\text{x}10^5$. The simulated data is all Poisson distributed and all assumed to be 64 radial bins and 64 angular views evenly spaced over 180^0. Projections are calculated mathematically.

The standard thorax test image is gray-scale image of size 128x128, with coverage angle ranging from 0 to 360 ^{o} with rotational increment of 2^o to 10^o. The resultant reconstructed image obtained from different algorithms is given in Fig. 3.9 & 3.12. For simulation study MATLAB 2013b software was used on PC with Intel(R) Core (TM) 2 Duo CPU U9600 @ 1.6GHz, 4.00 GB RAM, and 64 bit Operating system.

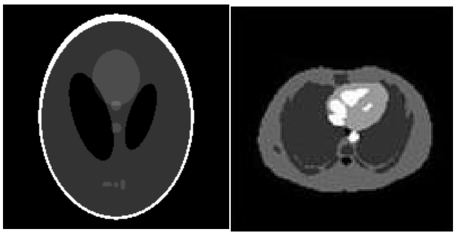

Fig 3.8: Modified Sheep-Logan mathematical phantom (64x64pixels) & Standard thorax medical image (128x128 pixels)

The performance of the proposed hybrid method (MLEM+AD) for image reconstruction defined by Equation (14) has been evaluated both qualitatively and quantitatively in terms of various performance measurements metrics such as: signal-to-noise ratio (SNR), the peak signal-to-noise ratio (PSNR), the correlation parameter (CP) (Rajeev *et. al.,* 2013), and mean structure similarity index map (MSSIM) (Rajeev *et. al.,* 2013). The SNR and PSNR give the error measures in reconstruction process. The correlation parameter (CP) is a measure of edge preservation in the reconstructed image. The MSSIM is a measure of preservation of luminance, contrast and structure of the image after the reconstruction process, which is necessary for medical images.

For implementation of the proposed method i.e. (MLEM+AD) algorithms Eq. (3.36) were used. A Poisson noise of magnitude 10% is added to projections. The value of Δt was set to 0.24 and value of conductivity coefficient k (kappa) was set to 0.033 to 1.0 for different test cases and within each MLEM step, AD is run for 3 iterations. The reconstructed images generated by different algorithms are shown in Fig.3.9 & 3.12. From the figures, we can see that the proposed algorithm has well performance of noise removal and edges preservation especially the thin edges and detail information. At the same time, we can observe that the MLEM+AD algorithm overcomes the shortcoming of streak artifacts and the reconstructed image is more similar to the original phantom.

For comparative analysis, the proposed and other standard algorithms were run for 1000 iterations to observe the convergence pattern. The algorithm is run for 1000 iterations and graphs are plotted for SNR, PSNR, CP, and MSSIM along with number of iterations for different algorithms which are shown in Figs. 3.10 and 3.13 for two different test cases. From Figs.3.10 and 3.13, it is observed that the SNR and PSNR values associated with the hybrid method is always higher than that produced by other algorithms such as traditional SART, MLEM and MRP methods which indicates that the hybrid framework significantly improves the quality of reconstruction in terms of SNR and PSNR. Further it is observed for both the test cases that the proposed method is producing better reconstructed image in 100-150 iterations whereas other methods are taking much higher number of iterations. Fig. 3.10 & 3.13 shows that the CP values of proposed method are higher and close to unity in comparison to other methods which indicate that the proposed method is also capable of preserving the fine edges and structures during the reconstruction process. Fig. 3.10 & 3.13 shows that the MSSIM values of proposed method is higher which indicate that better reconstruction, it also preserves the luminance, contrast and other details of the image during the reconstruction processes. Table 3.3-3.4; shows the quantification values of SNRs, RMSEs, PSNRs, and CPs. The comparison table indicates that the proposed reconstruction method produce images with prefect quality than other reconstruction methods in consideration. All the parameters show the same trends of MLEM+AD > MRP > MLEM > SART. Figure 3.11 and 3.14, shows the error analysis of the line profile at middle row for the test case. To check the accuracy of the proceeding reconstructions, line plots were drawn, where x-axis represents the pixel position and y-axis represents pixel intensity value. Line plots along the mid-row line through the reconstructions produced by different methods show that the proposed method can recover image intensity effectively in comparison to other methods.

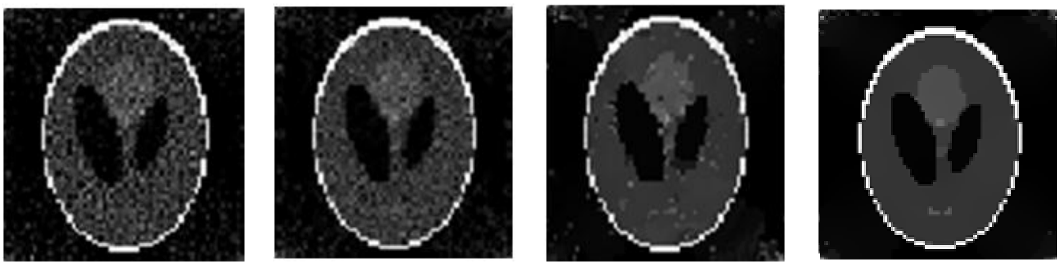

(a) **(b)** **(c)** **(d)**

Fig. 3.9: The modified Shepp-Logan phantom image reconstructed by different algorithms: (a) SART, (b) MLEM, (c) MRP, (d) MLEM+AD

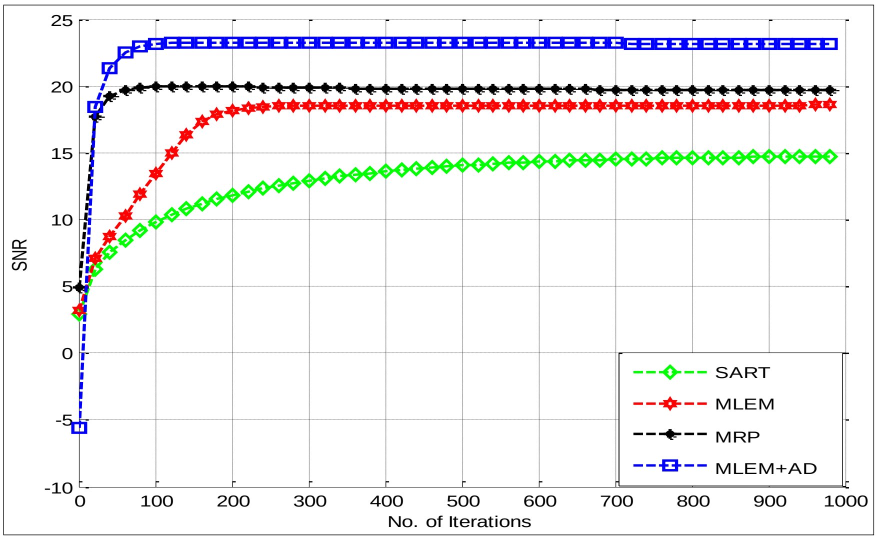

(a)

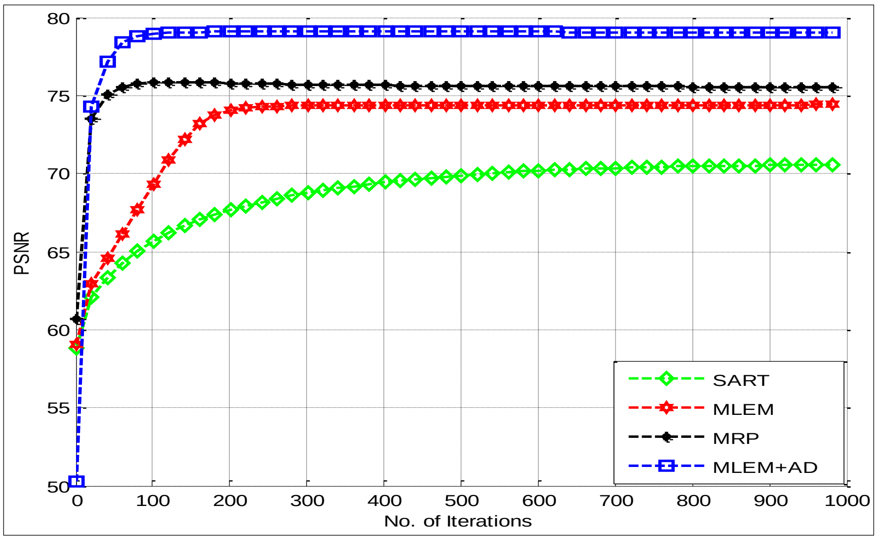

(b)

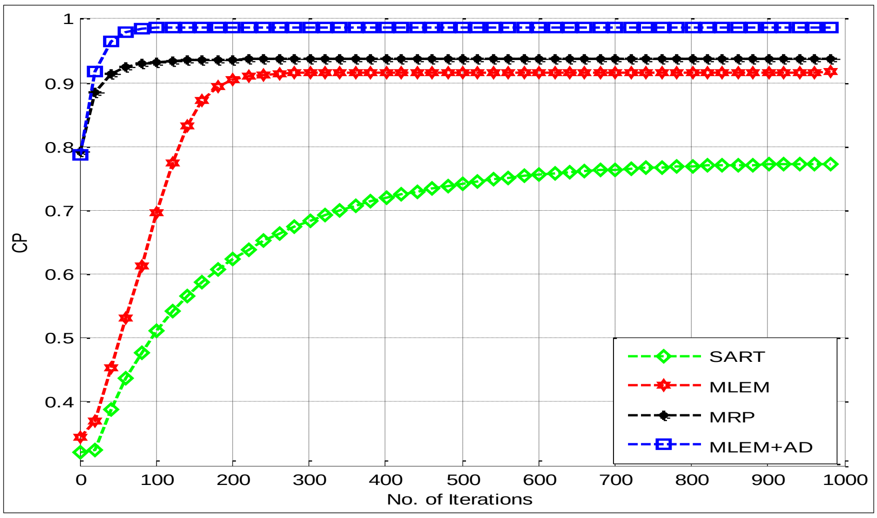

(c)

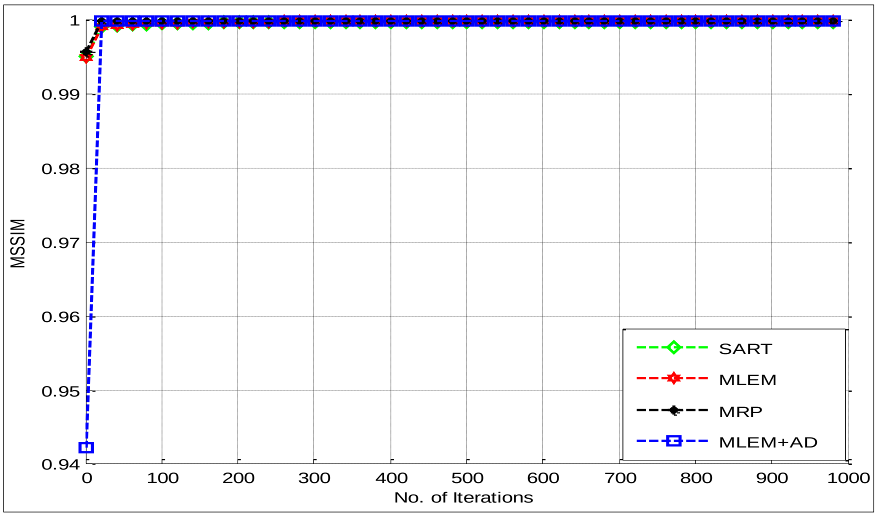

(d)

Fig.3.10: The Plots of (a) SNR, (b) PSNR, (c) CP, and (d) MSSIM along with No. of Iterations for different reconstruction algorithms.

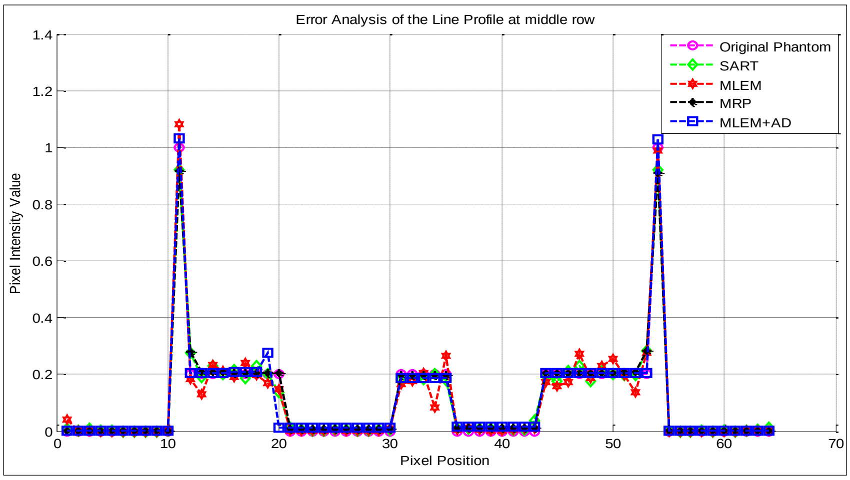

Fig. 3.11 Comparision of Line Plots of reconstructed Modified Shepp-Logan Phantom image using proposed (MLEM+AD) and other methods

Table 3.3: Performance measures for the reconstructed images of Test case 1

Performance Measures	SART	MLEM	MRP	(Proposed) MLEM+AD
SNR	14.7154	18.6479	19.7099	23.1723
PSNR	70.5598	74.4923	75.5543	79.0168
CP	0.7732	0.9178	0.9372	0.9864
MSSIM	0.9999	0.9999	0.9999	1.0000

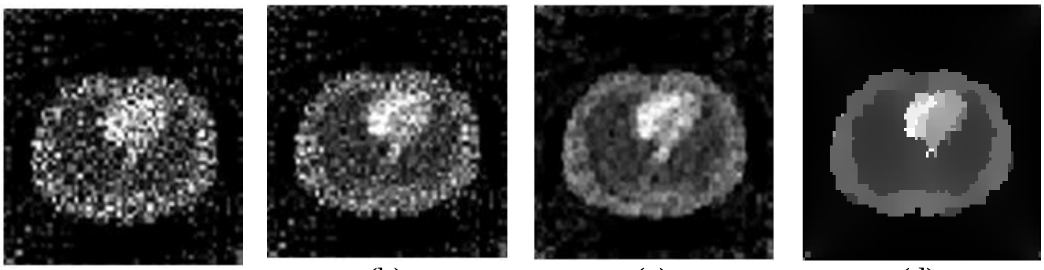

(a) (b) (c) (d)

Fig.3.12: The real thorax phantom image reconstructed by different algorithms: (a) SART, (b) MLEM, (c) MRP, (d) MLEM+AD

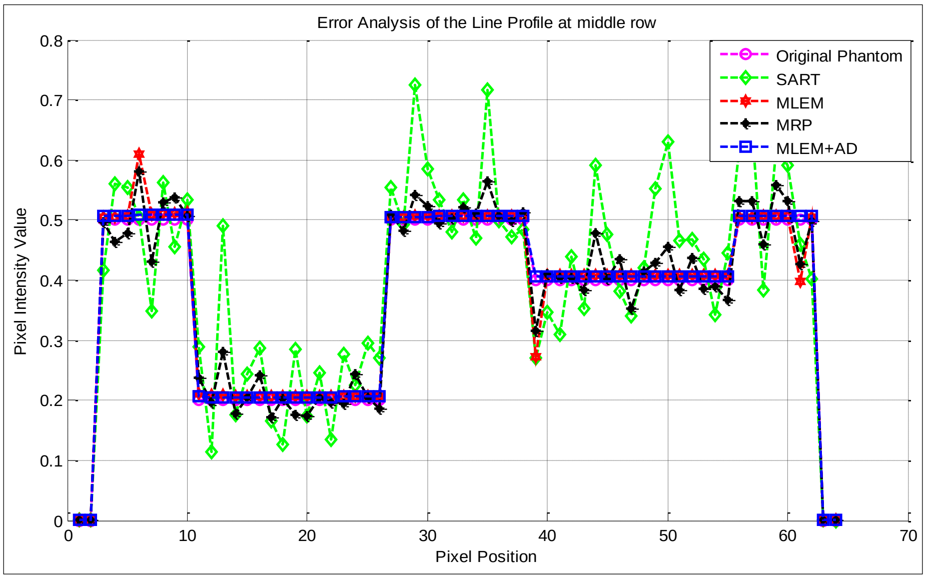

Fig. 3.14: Line Plot of standard Thorax phantom image

Table 3.4: Performance measures for thereconstructed images in Fig. 3.12

Performance Measures	SART	MLEM	MRP	(Proposed) MLEM+AD
SNR	13.2663	18.4005	19.2487	21.9977
PSNR	69.6957	74.8299	75.6781	78.4271
CP	0.7403	0.9336	0.9391	0.9863
MSSIM	0.9998	0.9999	0.9999	0.9999

Both the visual-displays and the line plots suggest that the proposed model is preferable to the existing reconstruction methods. In view of above analysis and discussions for above simulation study under consideration it is observed that the proposed hybrid iterative framework converges very fast, producing the better visual results having less reconstruction error, higher SNR values, better edge, structure, luminance, and contrast preservation capabilities in comparison to other standard methods in consideration.

3.4. Discussions

Statistical image reconstruction methods for Computed Tomography (CT), Positron Eemission Tomography (PET) and Single Positron Emission Computed Tomography (SPECT) play a significant role in the image quality by using spatial regularization that penalizes image intensity difference between neighboring pixels. The chapter introduced the most commonly used quadratic priors, which smooth's both high frequency noise and edge details, which tends to produce an unfavorable result while edge-preserving non-quadratic priors tends to produce blocky piecewise regions. However, these edges-preserving priors mostly depend on local smoothness or edges. It does not consider the basic fine structure information of the desired image, such as grey levels, edge indicator, dominant direction and frequency. To address the aforementioned issues of the conventional regularizations/priors, this chapter presented and evaluated a hybrid approach to regularize maximum likelihood expectation maximization (MLEM) iterative reconstruction technique with poisson variability.

In the second proposed model, regularization was achieved by penalizing MLEM with partial differential equation (PDE) diffusion based anisotropic diffusion (AD) prior to form hybrid method (MLEM+AD) that aim to impose an effective edge preserving and noise removing to optimize the quality of SPECT/PET reconstructed images. The measured data is corrupted by Poisson noise iteratively in the image domain. The proposed hybrid approach was more robust than the conventional regularization in differentiating sharp edges from random fluctuations due to noise. A comparative analysis of the proposed model with some other existing standard methods in literature was presented qualitatively and quantitatively using simulated test phantom and standard digital image. An experimental result indicates that the proposed method yields significantly improve in quality of the reconstructed images from the projection data. The obtained results justify the applicability of the proposed method. This method provides comparisons over using 1000 iterations; found that the proposed method provided much improved results. The proposed method needs fewer measurements to obtain a good high quality image, which result decrease in the missing or incomplete data problem. This method has shown to fetch better looking images, improved SNR values and reduced noise levels. For the case without regularization, the blurring and dislocating the useful edge information of images problem has been increased and the limit of the sequence of iterations is also increasing.

3.5. Conclusion

In this chapter, various priors have been studied and this chapter focuses on improving statistical iterative reconstruction algorithms by incorporating a suitable prior knowledge of the object being scanned. We have presented some statistical maximum likelihood (ML) based approach for CT, PET, and SPECT image reconstruction methods. The proposed method investigates and presents various choices of regularization priors used in standard SIR reconstruction methods like MLE, MRP, and OSEM in literature. Experimental analysis has been performed over own created mathematical test phantoms and benchmark Shepp-Logan head phantom plus real thorax test phantom. The results have been compared with existing methods using six quantitate measures that are signal-to-noise ratio (SNR), the root mean square error (RMSE), the peak signal-to-noise ratio (PSNR), the correlation parameter (CP), and mean structure similarity index map (MSSIM). Overcoming the undesirable effects with regularization will lead to smooth out and reduction in the reconstructed images. Therefore, proposed hybrid approach (called MLEM+AD) to regularize which dominates in CT images that improve the SNR values. The method has been easily extended to three dimensions. Future work includes faster implementation using parallel computing, graphical processing units (GPU's) and application to real data.